

Case Record of a Strut-free Excavation with Buttress Walls in Soft Soil

Aswin Lim^{1,2} and Chang-Yu Ou²

¹ Department of Civil and Construction Engineering, National Taiwan University of Science and Technology, Taipei 10672, Taiwan

aswin_lim@yahoo.co.id

² Department of Civil Engineering, Universitas Katolik Parahyangan, Bandung 40141, Indonesia

Abstract. This paper presents a well-documented strut-free excavation case with diaphragm walls, buttress walls, and partial floor slabs as the strut-free retaining system. The final excavation level was 9.2 m, covering an area about 17340 m². Because of its large excavation geometry, this project utilized the strut-free retaining system to reduce the construction cost and period. The soil layers above the final excavation level are dominated by the soft to medium clay layer (SPT = 2–7) and the loose silty sand layer (SPT = 2–6). According to the interpretation of field monitoring results, the following significant findings were drawn, such as (1) the measured maximum wall deflection was similar compared with strutted excavation case histories in the Taipei area. The maximum wall deflections to final excavation level ratio (δ_{hmax}/H_e) were between 0.27 and 0.55; (2) at the long-side of diaphragm wall, the pattern of the wall deflections is a cantilever shape with a translational movement at the wall toe and the location of maximum wall deflection was near the top of the wall; (3) at the short-side of diaphragm wall, the pattern of the wall deflections when reaching the final excavation level was a curvature shape and the location of maximum wall deflection was slightly lower than the final excavation level; (4) The maximum ground surface settlements to final excavation level ratio were below $\delta_{\text{vmax}}/H_e = 0.3\%$. Although it was quite small, the ground surface settlements extend to the significant distance behind the diaphragm wall; (5) the strut-free retaining system was proven successful to retain soil during excavation.

Keywords: Strut-free system · Buttress walls · Excavation · Soft soil

1 Introduction

In recent decades, buttress walls are widely adopted as an auxiliary measure for the protection of adjacent buildings during excavation in Taiwan (Ou et al. 2008; Hsieh et al. 2015; Hsieh et al. 2016; Hsieh et al. 2017). As an auxiliary measure, the diaphragm wall is mainly supported by steel struts (braced excavation method) and/or concrete floor slabs (top-down excavation method). Buttress walls are concrete walls perpendicular to the diaphragm wall with the limited length. In common practices, buttress walls could be located inside the excavation zone (the inner buttress wall) and/or outside the excavation zone (the outer buttress wall) (Lin and Woo 2007) as

illustrated in Fig. 1a. In addition, the shape of buttress walls could be the rectangular shape (R-shape), or the L-shape (Lim et al. 2016) as illustrated in Fig. 1b. Those kinds of buttress walls were used in the case history reported in this paper.

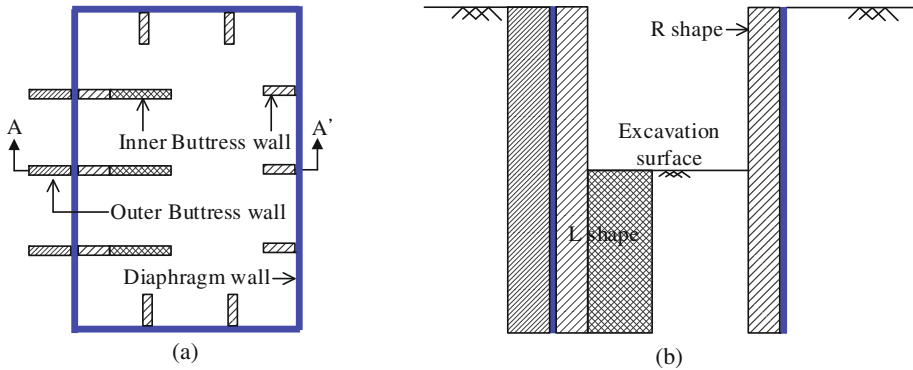


Fig. 1. Schematic diagram of buttress walls: (a) Plan view; (b) Cross-section A-A' view

Besides as an auxiliary measure, buttress walls are also used as main components in the strut-free retaining wall system. Chuah and Tan (2010) investigated the Tribeca excavation case in Singapore. The excavation geometry was about 75 m 52 m. The Tribeca excavation adopted the counterfort diaphragm wall system to retain 6.6 to 8 m depth of excavation in the Singapore Marine Clay. The retaining system consists of buttress walls combined with embedded diaphragm walls, and counterfort slabs. This system was successfully executed with the maximum wall deflection to final excavation level ratio (δ_{hmax}/H_c) equal to 1.33%, in which it was quite large compared with the common excavation methods.

The objective of this paper is to report the performance of a case history through field monitoring results. The main features of this case history are (1) the excavation geometry is very large, that is 195.7 m in length and 88.6 m in width, (2) the excavation adopted the strut-free retaining system, and (3) the subsurface conditions are dominated by soft soil.

2 Project Description and Instrumentation

The Xizhi excavation project is located in New Taipei City, Taiwan. The project is considered as a large excavation with the dimension of 195.7 m 88.6 m, and it was excavated to the depth of 9.2 m. It is an industrial building with two floors of basements, and 17 stories above ground. The basement was completed in 3 stages using the periphery top-down method in which floor slabs were casted with a limited width and were located at the excavation circumference. Furthermore, the buttress walls were maintained during the excavation process and demolished after completion of the lower structures. The excavation stages are summarized in Table 1.

Table 1. Construction sequence of excavation project

Stage	Date	Days	Construction activity
Initial	2008/11/20–2009/01/12	0–53	Construct diaphragm walls and buttress walls
	2009/01/12–2009/02/28	53–100	Install monitoring systems
1	2009/03/01–2009/10/28	100–342	Excavate to GL –1.5 m
			Construct partial first-floor slabs (1FL)
2	2009/10/29–2010/02/21	342–458	Excavate to GL –5.0 m
			Construct partial first basement slabs (B1F)
3	2010/02/22–2010/07/28	458–615	Excavate to GL –9.2 m

In addition, the earth retaining system consists of 20.5 m depth of diaphragm walls (0.5 m thick) with several types of buttress walls (0.5 m thick) as depicted in Fig. 2. The spacing between the buttress walls is around 8.5 m and the length of the buttress walls was varied between 4.8 m to 9.7 m. The diaphragm walls, the buttress walls, and the partial floor slabs were casted using concrete with $f'_c = 27.45$ MPa. Moreover, the diaphragm wall and the buttress walls were not founded in the hard-stratum (NSPT > 50). Moreover, deflections of diaphragm wall were measured by eleven in-wall inclinometer casings (SID 01 to SID 11), 25.5 m in depth. Ground surface settlements were measured at five sections perpendicular to the diaphragm wall with settlement markers (SM 01, SM 03, SM 04, SM 05, and SM 07), which was attached to the ground, as shown in Fig. 2.

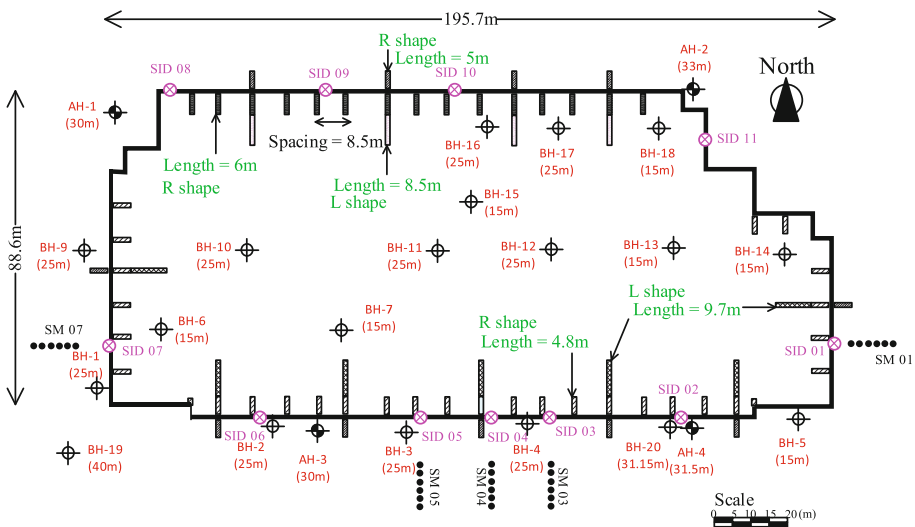


Fig. 2. Excavation geometry and monitoring layout

3 Ground Conditions

The excavation site is located at the terrace deposit of Keelung River which mainly comprises of clay and silty sand layers. In total, twenty initial boreholes (BH-1 to BH-20) and four additional boreholes (AH-1 to AH-4) with various depths were drilled to examine the profile of subsurface soils (Fig. 2). The groundwater level observed during additional boring was located about 10 m below the ground surface. Hence, no dewatering scheme was planned. The ground conditions and soil properties at the site have been investigated by a series of field tests (e.g., standard penetration tests) and laboratory tests (e.g., oedometer tests and triaxial tests). Figure 3 shows the soil profiles and measured soil properties.

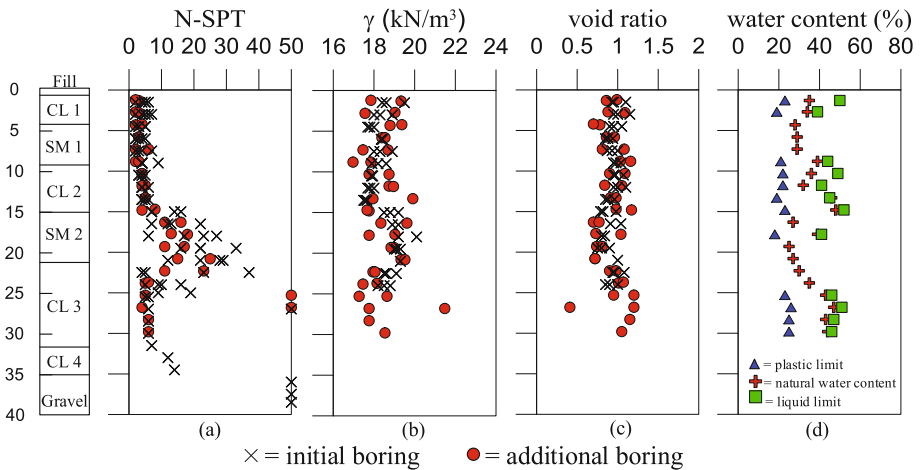


Fig. 3. Profiles of (a) N-SPT values, (b) soil unit weight, (c) void ratio, and (d) Atterberg limits for the project site

The strata of the site could be divided into eight idealized layers. From top to bottom, they are described as follows:

1. The first layer (GL 0–GL –1.0 m) is a layer of fill material which consists of gravels, silty clays, and bricks. The unit weight of this layer is about 19 kN/m^3 .
2. The second layer (GL –1 to GL –4.0 m) is a layer of gray silty clay (CL 1), with N_{SPT} values varying from 2 to 7. Its average total unit weight is about 18 kN/m^3 , void ratio between 0.8 and 1.1, average natural water content about 34%, liquid limit between 39 and 50, plasticity limit between 19 and 23, compression index (C_c) is 0.3, swelling index (C_s) is 0.03, effective friction angle is about 26° to 28° .
3. The third layer (GL –4 m to GL –9 m) is a silty sand layer (SM 1). The N_{SPT} values varied from 2 to 6 and the average unit weight is 18.5 kN/m^3 . Its effective friction angle is about 28° and its natural water content is about 30% to 40%.

4. The fourth layer (GL -9 m to GL -15 m) is a layer of gray silty clay (CL 2), with N_{SPT} values varying from 2 to 9. Its average total unit weight is about 18.2 kN/m^3 ; average void ratio is 1.04 (GL -9 m to GL -13 m) and 1.08 (GL -13 m to GL -15 m); average natural water content about 40%, liquid limit between 40 and 50, plasticity limit between 20 and 25, compression index (C_c) is 0.3, swelling index (C_s) is 0.03, effective friction angle is about 28° .
5. The fifth layer (GL -15 m to GL -22 m) is a silty sand layer (SM 2). The N_{SPT} values varied from 8 to 38 and the average unit weight is 18.9 kN/m^3 . Its effective friction angle is about 32° and its natural water content is about 22% to 30%.
6. The sixth layer (GL -22 m to GL -32 m) is a layer of silty clay (CL 3), with N_{SPT} values varying from 4 to 10. Its average total unit weight is about 17.7 kN/m^3 , average void ratio is 1.16, natural water content between 30% to 45%, liquid limit between 45 and 50, plasticity limit between 23 and 25, compression index (C_c) is 0.2, swelling index (C_s) is 0.02, and effective friction angle is about 30° .
7. The seventh layer (GL -32 m to GL -35 m) is a layer of silty clay (CL 4), with N_{SPT} values varying from 12 to 14. Its average total unit weight is about 17.7 kN/m^3 , compression index (C_c) is 0.2, swelling index (C_s) is 0.02, and effective friction angle is about 31° .

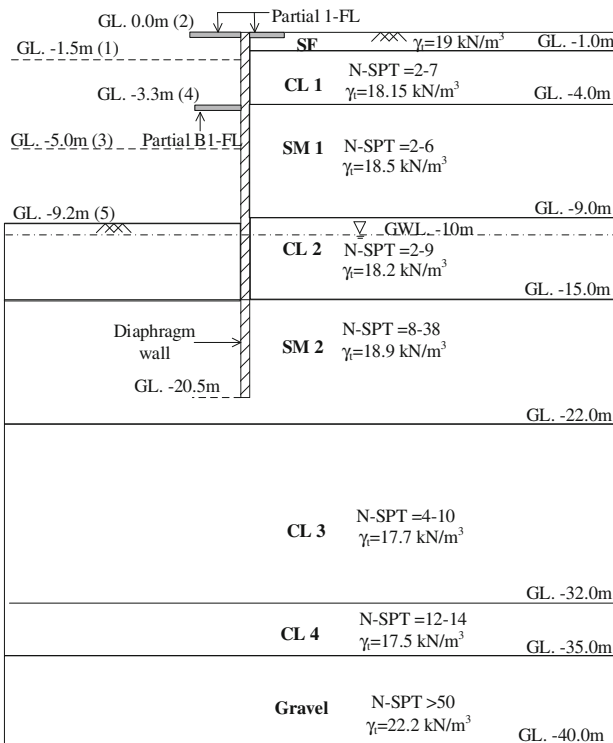


Fig. 4. Excavation and subsurface profile

8. The eighth layer (GL -35 m to -40 m) is a layer of gray gravels (GW). The N_{SPT} values are larger than 50 and the average unit weight is 22.2 kN/m^3 . Its effective friction angle is about 38° .

Furthermore, the profile of the subsurface soils and the excavation sequences is illustrated in Fig. 4.

4 Field Monitoring Results and Discussion

The diaphragm wall deflections and its corresponding ground surface settlements at the south side are represented by SID 04, SID 05, SM 04, and SM 05, respectively. In general, the pattern of the wall deflections is a cantilever shape with a translational movement at the wall toe because the toe of the diaphragm wall was not founded in the hard-stratum, as plotted in Figs. 5 and 6. The cantilever shape of wall deflections was also observed by Chua and Tan (2010) in their reported case. It should be noted that the length of the south diaphragm wall is 195.7 m and the location of those inclinometers was close to the center of the diaphragm wall. According to Ou et al. 1996, the plane strain ratio (PSR) was equal to unity. Thus, the measured results could be judged that they were less affected by the corner effect, or more likely in the plane strain condition. In such a condition, it seems that the first partial floor slabs did not function for restraining wall deflections at the top of the diaphragm wall, but the function was more likely similar to a capping beam where it distributed the wall deflection more uniformly at the top of the diaphragm wall. The similar wall deflection shape was also observed at the north side, but with smaller magnitude, as shown in Fig. 7. The smaller magnitude

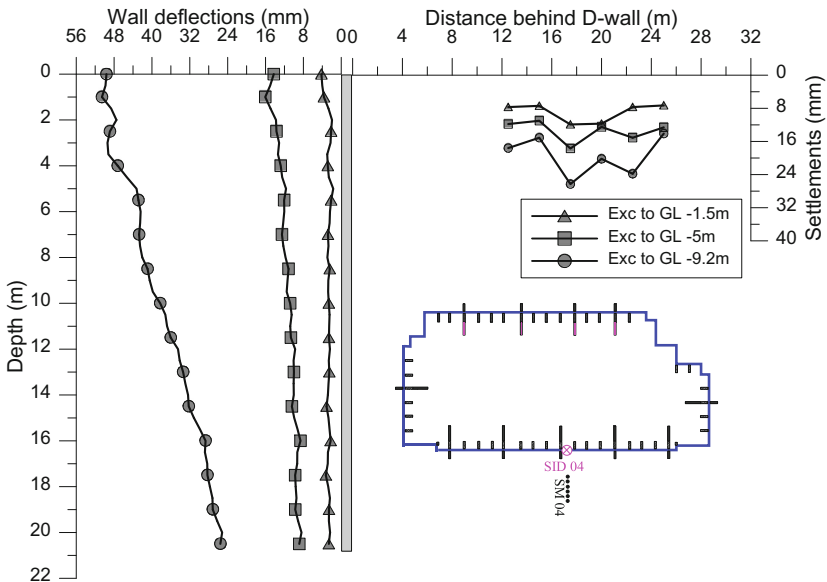


Fig. 5. Measured wall deflections and ground surface settlements of SID 04 and SM 04

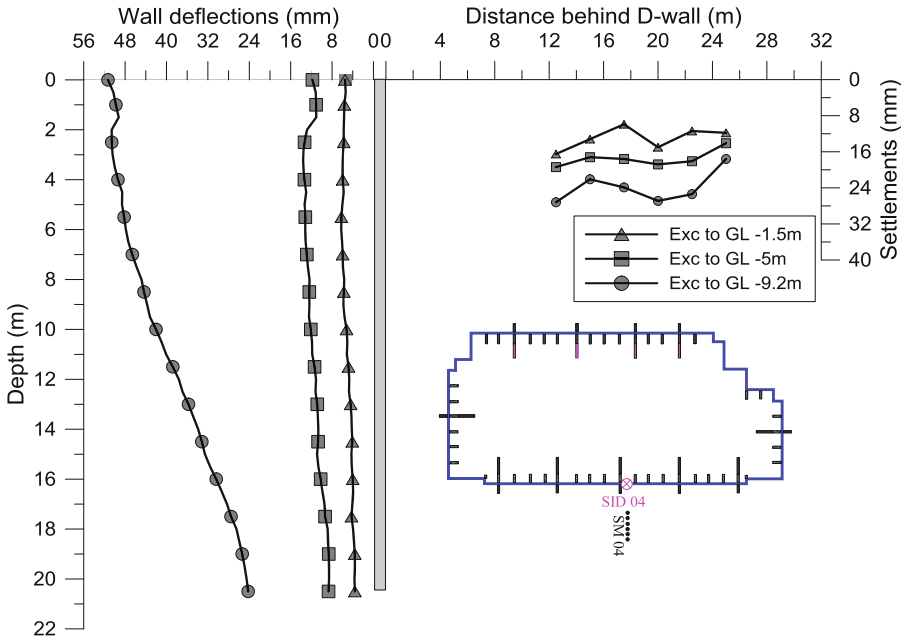


Fig. 6. Measured wall deflections and ground surface settlements of SID 05 and SM 05

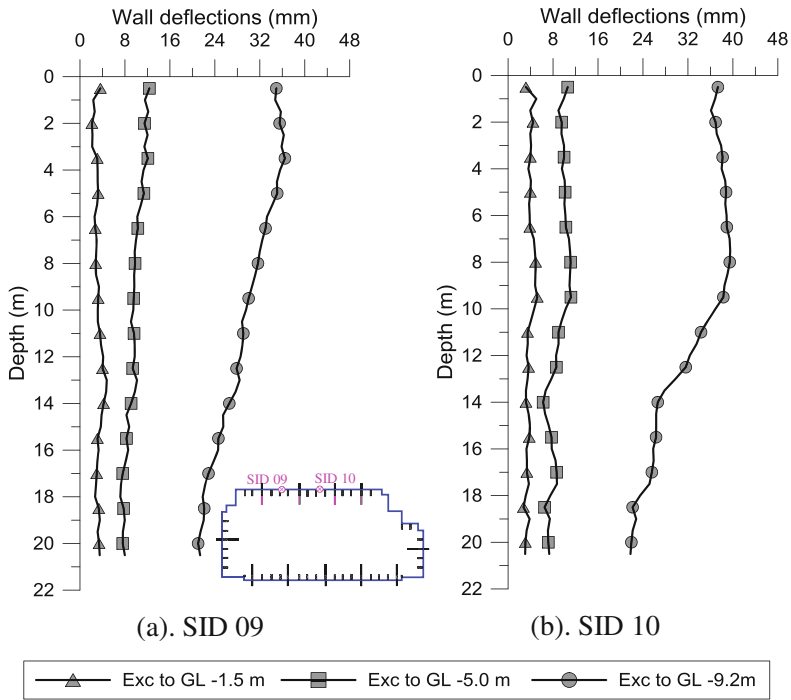


Fig. 7. Measured wall deflections of SID 09 and SID 10

of diaphragm wall deflections was contributed from the subsoil conditions at the north side was stiffer than the south side, especially the CL 1 layer. The N-SPT of CL 1 layer at the north side was 5, meanwhile, the CL 1 layer at the south side was 2. Obviously, the magnitude of wall deflections at the north side was smaller than the magnitude of wall deflections at the south side, and the location of maximum wall deflection was near the top of the wall.

Furthermore, the diaphragm wall deflections and its corresponding ground surface settlements at the west and the east sides are represented by SID 07, SID 01, SM 07, and SM 07, respectively. In general, the pattern of the wall deflections at the final stage is a curvature shape, as depicted in Figs. 8 and 9. It should be noted that the length of the west and east diaphragm wall is 65 m and 50 m, respectively, and the location of those inclinometers was 20 m away from the corner of the diaphragm wall. According to Ou et al. 1996, the PSR of SID 07 and SID 01 were equal to 0.45 and 0.35, respectively. Thus, the measured results could be judged that they were much affected by the corner effect. In such a condition, it seems that the combination of the corner effect and first partial floor slabs could restraint wall deflections at the top of the diaphragm wall. The location of maximum wall deflection was slightly lower than the final excavation level when the shape of the wall deflections was a curvature. Moreover, Table 2 summarizes all of the maximum wall deflection at various excavation stages and locations.

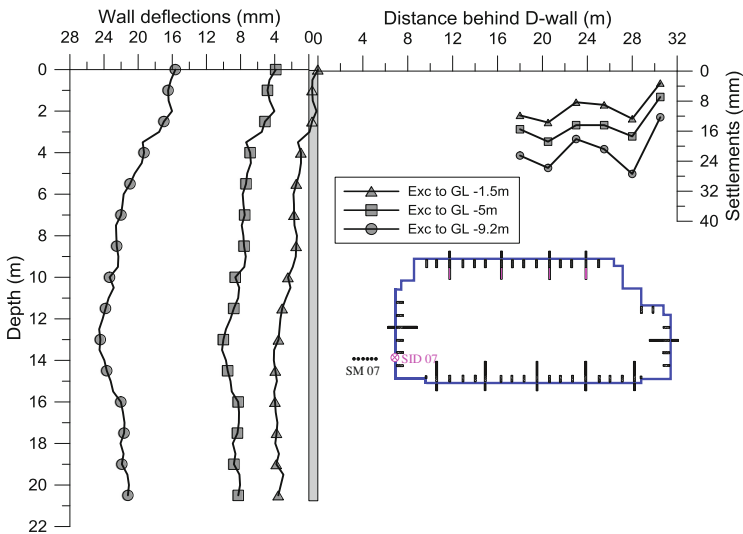


Fig. 8. Measured wall deflections and ground surface settlements of SID 07 and SM 07

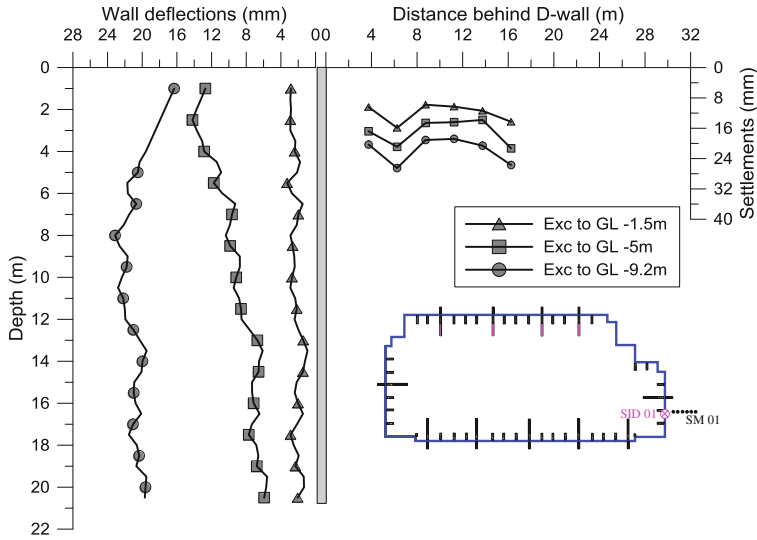


Fig. 9. Measured wall deflections and ground surface settlements of SID 01 and SM 01

Table 2. Summary of maximum wall deflection at various excavation stages and locations

Depth of excavation	Maximum wall deflection (unit: mm)										
	SID 01	SID 02	SID 03	SID 04	SID 05	SID 06	SID 07	SID 08	SID 09	SID 10	SID 11
GL -1.5 m	10.8	7.0	3.8	4.2	6.2	12.4	4.1	3.6	6.5	5.2	5.5
GL -5.0 m	20.9	13.2	9.7	16.1	13.6	18.2	10.2	16.4	15.8	11.2	15.0
GL -9.2 m	25.4	30.3	41.4	50.6	51.3	46.1	24.6	30.8	37.4	39.5	33.6

Figure 10 presents the relationship between measured maximum wall deflection, δ_{hmax} , and final excavation level, H_e . Field data from some published case histories in Taipei Clay (Ou et al. 1993) and Singapore Clay (Chuah and Tan 2010) are also included. It should be noted that the Taipei cases were adopted common excavation methods (i.e. braced excavation or top-down excavation method), meanwhile the Singapore case was adopted the counterfort diaphragm wall system (also a kind of strut-free retaining system). In this project, the maximum wall deflections fell between 0.27 and 0.55% H_e , where the lower and upper values indicate the deflection of diaphragm wall near the corner and the center (PSR = 1.0) of diaphragm wall, respectively. It is quite surprisingly that the maximum wall deflection of the strut-free retaining system was in the range of the maximum wall deflection obtained from common excavation methods (i.e. braced excavation or top-down excavation method). Meanwhile, the Singapore case yielded the maximum wall deflection to final excavation level ratio was 1.33%. For the Singapore case, the groundwater level was near the ground surface level, but the groundwater level was below the final excavation level for this project (Fig. 4). Hence, the possible reason of the relatively small maximum

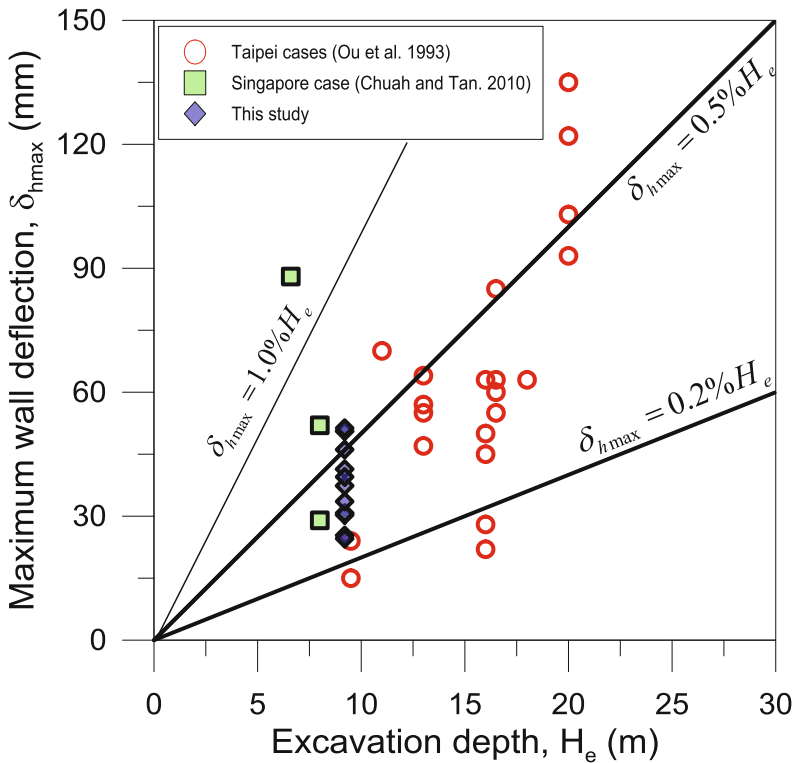


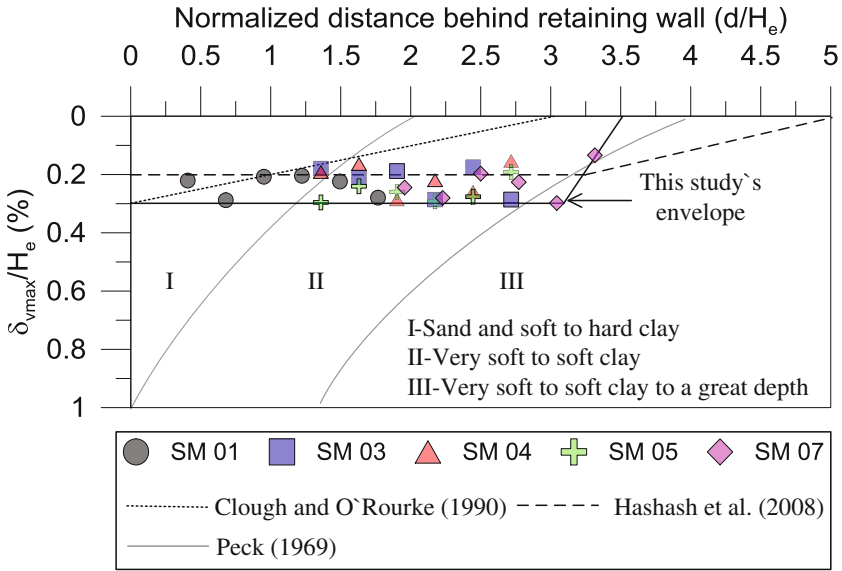
Fig. 10. Relationships between maximum wall deflections and excavation depth

wall deflections measured from this project was the absence of water pressure acting on the strut-free retaining system (from GL -0.0 m to GL -10 m).

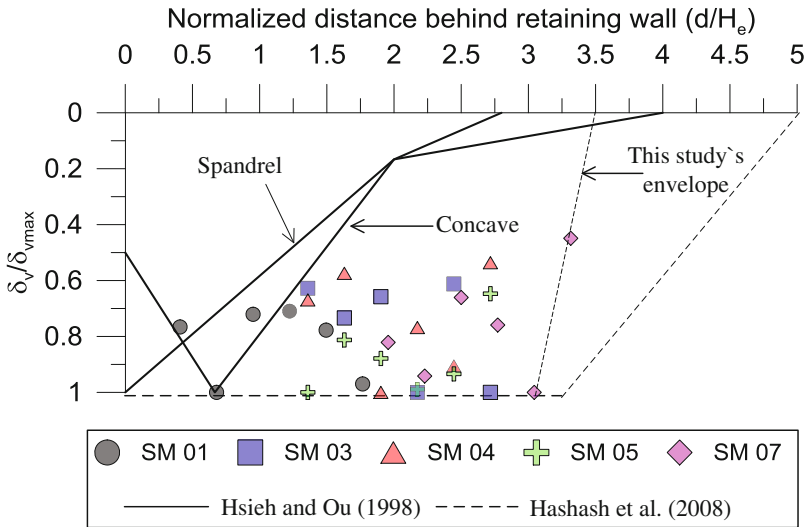
Figures 5, 6, 8, and 9 present the ground settlement profiles of SM 04, SM 05, SM 07 and SM 01, respectively. A positive value indicates settlement. Generally, ground surface settlements increased as excavation proceeded downward. The measured data show that the maximum settlement for all the measured data is about 27 mm and that settlements extend as far as 30 m behind the wall, although the data are scarce from 0 to 12 m behind the wall. The ground surface settlements at various excavation stages and locations are listed in Table 3. The measured maximum ground surface settlements were

Table 3. Summary of ground surface settlement at various excavation stages and locations

Depth of excavation	Maximum ground surface settlement (unit: mm)				
	SM 01	SM 03	SM 04	SM 05	SM 07
GL -1.5 m	16	15	12	17	14
GL -5.0 m	21	20	18	19	19
GL -9.2 m	27	26	26	27	27



(a)



(b)

Fig. 11. Measured ground surface settlement profiles versus those predicted by empirical methods: (a) relationship between normalized ground settlements and normalized distance from wall; (b) relationship between relative ground settlements and normalized distance from wall

about 0.3% of final excavation level (H_e), and they were among those concluded by Clough and O'Rourke (1990) for excavation in clay with the boundary 0.15%–0.5% H_e .

Figure 11a depicts the normalized ground surface settlements versus normalized distance behind the excavation. Both quantities are normalized with respect to final excavation level. Most of the measured data were located within the Zone II proposed by Peck (1969) and also slightly below those predicted by Hashash et al. (2008) for medium clay and Clough and O'Rourke (1990) for stiff clay. Although most maximum settlements are less than $\delta_{vmax}/H_e = 0.03\%$, the normalized settlements extend to distances about 3.5 H_e .

Figure 11b shows the relationship between relative ground surface settlement, δ_v/δ_{vmax} , and normalized distance, d/H_e , where δ_v is the ground surface settlement at a certain distance behind diaphragm wall, and δ_{vmax} is the maximum ground settlement along a section. The measured data show that no clear spandrel or concave shapes of the ground surface settlement was observed, rather than it appears that most ground surface settlements fell in the envelope introduced by Hashash et al. (2008) but with smaller normalized distance (d/H_e). The measurements show that even for distances up to 1.5–3 H_e , the settlements are on the order of 60% of maximum settlements.

In this study, the envelopes for the clay profiles describe the lower settlement ratios but the wider distribution of settlements behind the wall. For the clay profiles, the envelopes reflect a limit on the lateral extent of settlements to a distance ratio of 3.5. Some of the possible reasons for this settlement characteristic were (1) It seems that the soil behavior is more linear because the relatively small deformations experienced by the soil, (2) Construction activities near the settlement markers might have some effects on measured settlements at distances far away from the excavation.

5 Conclusions

Through a comprehensive instrumentation program, the monitored results of this strut-free large excavation project in soft clay have been interpreted and discussed. Based on the field monitoring results, several conclusions could be drawn:

1. The excavation was successfully constructed with the strut-free retaining system, where buttress walls were integrated with the diaphragm walls and maintained during the excavation process.
2. The measured maximum wall deflection was similar compared with strutted excavation case histories in the Taipei area. The maximum wall deflections to final excavation level ratio (δ_{hmax}/H_e) were between 0.27 and 0.55.
3. At the long-side of diaphragm wall, the pattern of the wall deflections is a cantilever shape with a translational movement at the wall toe and the location of maximum wall deflection was near the top of the wall. Meanwhile, at the short-side of diaphragm wall, the pattern of the wall deflections when reaching the final excavation level was a curvature shape and the location of maximum wall deflection was slightly lower than the final excavation level. It seems that the corner effect played significant roles in determining the magnitude and the shape of wall deflections.

4. The maximum ground surface settlements to final excavation level ratio were below $\delta_{vmax}/H_c = 0.3\%$. Although it was quite small, the ground surface settlements extend to the significant distance behind the diaphragm wall (up to $3.5 \times$ final excavation level).

Acknowledgment. The authors acknowledge the support provided by the Ministry of Science and Technology in Taiwan via grant number MOST103-2221-E-011-070-MY3. The authors would like to thank Sino Geotechnology, Inc. for the provision of detailed geotechnical information on the case study.

References

- Chuah, S.S., Tan, S.A.: Numerical study on a new strut-free counterfort embedded wall in Singapore. In: Earth Retention Conference, pp. 740–747 (2010)
- Clough, G.W., O'Rourke, T.D.: Construction induced movement of in-situ walls. Geotechnical Special Publication: Design and Performance of Earth Retaining Structures (GSP 25), pp. 439–470. ASCE, Reston (1990)
- Hashash, Y., Osouli, A., Marulanda, C.: Central artery/tunnel project excavation induced ground deformations. *J. Geotech. Geoenviron. Eng.*, 1399–1406 (2008). doi:[10.1061/\(ASCE\)1090-0241\(2008\)134:9\(1399\)](https://doi.org/10.1061/(ASCE)1090-0241(2008)134:9(1399))
- Hsieh, P.G., Ou, C.Y.: Shape and ground surface settlement profiles caused by excavation. *Can. Geotech. J.* **35**(6), 1004–1017 (1998)
- Hsieh, P.G., Ou, C.Y., Lin, Y.K., Lu, F.C.: Lesson learned in design of an excavation with the installation of buttress walls. *J. GeoEngin.* **10**(2), 63–73 (2015)
- Hsieh, P.G., Ou, C.Y., Hsieh, W.H.: Efficiency of excavations with buttress walls in reducing the deflection of the diaphragm wall. *Acta Geotech.* **11**(5), 1087–1102 (2016)
- Hsieh, H.S., Huang, Y.H., Hsu, W.T., Ge, L.: On the system stiffness of deep excavation in soft clay. *J. GeoEngin.* **12**(1), 21–34 (2017)
- Lim, A., Hsieh, P.G., Ou, C.Y.: Evaluation of buttress wall shapes to limit movements induced by deep excavation. *Comput. Geotech.* **78**, 155–170 (2016)
- Lin, D.G., Woo, S.M.: Three dimensional analyses of deep excavation in Taipei 101 construction project. *J. GeoEngin.* **2**(1), 29–41 (2007)
- Ou, C.Y., Hsieh, P.G., Chiou, D.C.: Characteristics of ground surface settlement during excavation. *Can. Geotech. J.* **30**, 758–767 (1993)
- Ou, C.Y., Chiou, D.C., Wu, T.S.: Three-dimensional finite element analysis of deep excavations. *J. Geotech. Eng.* **122**(5), 337–345 (1996)
- Ou, C.Y., Teng, F.C., Seed, R.B., Wang, I.W.: Using buttress walls to reduce excavation-induced movements. *Proc. Inst. Civ. Eng. Geotech. Eng.* **161**(GE4), 209–222 (2008)
- Peck, R.B.: Deep excavation and tunneling in soft ground: state-of-the-art-report. In: Proceeding of 7th International Conference of Soil Mechanics and Foundation Engineering (ISSMGE), pp. 225–281 (1969)